

# AGARD

ADVISORY GROUP FOR AEROSPACE RESEARCH & DEVELOPMENT

7 RUE ANCELLE, 92200 NEUILLY-SUR-SEINE, FRANCE

---

AGARD CONFERENCE PROCEEDINGS 582

## Remote Sensing:

## A Valuable Source of Information

(la Télédétection — source précieuse de renseignements)

*Papers presented at the Sensor and Propagation Panel Symposium, held in Toulouse, France  
22-25 April, 1996.*



**NORTH ATLANTIC TREATY ORGANIZATION**

---

Published October 1996

*Distribution and Availability on Back Cover*

## Remote Sensing by Active and Passive Optical Techniques

C. R. Philbrick, M. D. O'Brien, D. B. Lysak, T. D. Stevens and F. Balsiger

Electrical Engineering Department, and  
Remote Sensing Department, Applied Research Laboratory  
Penn State University  
State College, PA 16804 USA

### 1. SUMMARY

Active optical remote sensing techniques based on lidar have been mostly limited to ground based and aircraft applications because of rather restrictive  $1/R^2$  dependence of signal, low power efficiency (~1%) of flash lamp pumped lasers and large physical size required by the power system. The advances in diode pumped lasers and other electro-optical instruments make it possible to consider new possibilities. Opportunities for future aircraft, RPV and satellite platform measurements over large spatial scales have prompted us to evaluate current capabilities for ground-based lidar measurements with a view toward future compact lidars. We have examined the Raman and DIAL lidar techniques to determine their capability for various remote sensing applications. The Raman techniques, even with inherent sensitivity disadvantages of small scattering cross-sections, have proven to be highly successful for ground-based remote sensing because they easily provide quantitative results, and these techniques will still be valuable from aircraft altitudes. Examples of ground-based lidar measurements of structure properties and minor species profiles have been used to provide confidence in the model calculations of expected performance from flight platforms. Use of acousto-optical tunable filters (AOTF) with lidar techniques provide special capabilities for measurement of Raman and fluorescent lidar returns. Applications of SPR-DIAL techniques for high altitude platforms would be useful for detection of chemical pollution in the atmosphere and waterways. Capabilities of current ground-based lidar systems for profiling meteorological properties, such as: density, temperature, water vapor, refractivity, chemical species, aerosol extinction and particle characteristics, provide the base from which we may consider future applications. Our recent reports have described the capability of lidars to measure species and temperature profiles, this paper focuses on the ability of lidar to measure and quantify aerosol properties.

### 2. INTRODUCTION

Use of LIDAR sensor systems for atmospheric characterization is becoming an established technology.

Ground-based lidar using Raman, DIAL (Differential Absorption Lidar) and Doppler lidar techniques have demonstrated capabilities for remote sensing of all of the meteorological properties measured by standard radiosonde balloons. The flight of the NASA LITE experiment on the US space shuttle in 1994 (Ref 1) and the Russian-French lidar on the Mir Station in 1996 (Ref 2) provided major steps toward the eventual use of lidar at satellite altitudes. There are now many laboratories involved in lidar development, and advances are rapidly being made in materials and hardware. At ARL/PSU, we have developed and demonstrated several ground-based systems capable of measuring water vapor profiles, aerosol distribution and temperature profiles in the troposphere, stratosphere and mesosphere (Ref 3, 4, 5, 6). We are currently developing an operational prototype of a lidar system, Lidar Atmospheric Profile Sensor (LAPS), which will provide real time profiles of RF refractivity from measured profiles of temperature and water vapor (Ref 7). Use of Raman scattering and DIAL measurements to detect the spectra of several atmospheric pollution species and various chemical species has been examined (Ref 8). A multi-wavelength lidar instrument has demonstrated measurements of atmospheric pollutants and gas species using the SPR-DIAL technique with about sixty of the  $\text{CO}_2$  laser lines in the  $10\mu$  region of the spectrum (Ref 9).

Capabilities of lidar, combined with passive optical remote sensing techniques provide the basis for future sensor systems to measure atmospheric pollution episodes and for real time monitoring of industrial processes. Detection and profiling of chemical species in the atmosphere have been a long term goal of lidar techniques, however, manufacture of reliable and stable lasers, development of measurement techniques, and preparation of specialized filters have delayed progress toward the autonomous instrument which would be useful in many applications of lidar. The LAPS instrument program is one of the current activities which has the goal of developing an operational lidar system.

### 3. LIDAR BACKGROUND

During the past twenty years, researchers at several laboratories have demonstrated that lidar is capable of measuring many different properties of the atmosphere. The first Raman measurements of atmospheric properties with lidar were carried out in the late 1960's by Leonard (Ref 10) and Cooney (Ref 11). Two years later Melfi, et al. (Ref 12) and Cooney (Ref 13, 14) showed that it was possible to detect atmospheric water vapor using the Raman lidar technique. Inaba and Kobayasi (Ref 15) suggested several species that could be measured using vibrational Raman techniques. While these early tests showed that it was possible to measure the water vapor with limited range and accuracy, recent investigations have demonstrated significant improvements. Particularly, the investigations of Vaughan et al. (Ref 16), Melfi et al. (Ref 17), Whiteman et al. (Ref 18) and Philbrick et al. (Ref 19) have demonstrated rather convincingly that the Raman technique has an excellent capability for making accurate water vapor measurements, both during the day and night. A most useful review of the Raman and DIAL lidar techniques applied to water vapor measurement has been prepared by Grant (Ref 20).

### 4. LIDAR INSTRUMENT DEVELOPMENT

#### 4.1 LAMP Lidar

The LAMP (Lidar Atmospheric Measurements Program) lidar, which was developed at PSU in 1990, has been used during the past several years for atmospheric measurements using Raman vibrational and rotational scattering (Ref 19). Two detector systems have been prepared for the instrument. Initial measurements used a high altitude detector designed to cover the altitude range from 2 to 80 km. During the past 4 years, measurements have been focused on the troposphere with emphasis from the surface to 5 km, and several campaigns have been carried out which demonstrate the performance of Raman lidar

techniques compared with standard rawinsonde balloon measurements. Investigations have emphasized water vapor and molecular nitrogen profiles which are determined from the 1st Stokes vibrational Raman transitions from laser wavelengths of 532 nm, 355 nm and 266 nm. Profiles of the N<sub>2</sub> vibrational Raman scatter provide true extinction measurements in the lower atmosphere, provided that the optical depth is sufficiently small that multiple scattering can be neglected. Water vapor profiles are obtained from the ratio of signals measured at the following wavelength pairs: 660/607, 407/387 and 295/284. The fact that the profile is determined from a ratio removes most of the errors in the profiles and makes the technique preferred for many applications. Temperature structure has been measured using rotational Raman scattering in the anti-Stokes region between 526 and 532 nm. Table I summarizes the LAMP lidar characteristics. Several reports (for example, Ref 3, 4, 7, 19) have shown examples of water vapor and temperature profiles obtained using the LAMP lidar. Measurements have proven the capability of Raman lidar to obtain profiles of atmospheric structure properties and water vapor in the lower atmosphere during night conditions. By comparing the molecular profiles of the N<sub>2</sub> Raman and rotational Raman with the neutral atmosphere density gradient, which can be determined from the temperature profile, the optical extinction profile can be obtained. Daytime measurement capabilities have been demonstrated using the "solar blind" region from the 266 nm fourth harmonic of Nd:YAG. Daytime measurements of water vapor are determined using the Raman scatter ratio of 295/284 ultraviolet wavelengths. A correction must be applied to this ratio because of the absorption due to tropospheric ozone. The ratio of the O<sub>2</sub> to N<sub>2</sub> vibrational Raman measurements (277/284) on the slope of the Hartley band of ozone provides a DIAL measurement of the ozone profile in the lower atmosphere, from the surface to altitudes between 2 and 3 km.

Table 1. LAMP Lidar characteristics

Transmitter	Continuum NY-82 -- 20 Hz 5X Beam Expander	400 mj @ 532 nm 80 mj @ 266 nm
Receiver	41 cm Diameter Telescope	Fiber optic transfer
Detector	Eight PMT channels Photon Counting	528 and 530 nm -- Rotational Raman Temperature 660 and 607 nm -- Vibrational Raman Water Vapor 295 and 285 nm -- Daytime Water Vapor 277 and 284 nm -- Raman/DIAL Ozone
Data System	DSP 100 MHZ	75 meter range bins

## 4.2 LAPS Lidar

The Lidar Atmospheric Profile Sensor (LAPS) instrument is currently undergoing tests of its automated operation to determine its performance under a wide range of meteorological conditions. The instrument measures water vapor profiles based on the vibrational Raman scattering and the temperature profile based on the rotational Raman scattering. These measurements are used to calculate real-time profiles of RF refractivity. Profiles are obtained each 5 minutes with a vertical resolution of 75 meters (efforts are underway to improve the resolution to 15 meters) from the surface to 7 km. The prototype instrument, which includes several sub-systems to automate and monitor the operation, has been designed to provide the real-time measurements of profiles. The instrument includes an X-band radar which detects aircraft as they approach the beam and automatically protects a 6 degree cone angle around the beam. The instrument includes calibration, performance testing and built-in-tests to check many functions. The larger laser and telescope of the LAPS instrument yield a signal approximately ten times that of the LAMP instrument.

## 4.3. Acousto-optical Tunable Filter

Remote sensing systems with high spectral resolution in the visible and near-IR regions can provide the sensitivity and discrimination against interferences and monitor the hazardous chemical vapors in the background environment. Due to their compact size, ruggedness and relatively narrow spectral resolution, Acousto-Optical Tunable Filters (AOTF) provide the opportunity to select the Raman line of a species of interest. Current state of the art AOTF instruments are capable of a spectral resolution of better than  $10 \text{ cm}^{-1}$  at selected visible/uv wavelengths (0.3 nm at 500 nm). The advantages in using the Raman signals to measure chemical species which exist in significant concentrations in the lower atmosphere are clear.

In particular, Raman lidar measurements provide the accurate concentration measurements of species from the signal ratio when simple corrections are made for the optical extinction, which is also derived from the measurements. Examples of the many species that could be measured, using a filter with a narrow band-pass, typically 0.2 nm, are indicated in summary references (Ref 15, 21). An AOTF (Ref 22, 23) is being combined with Raman lidar to enable the operator to select any vibrational Raman line to measure the spectral signatures of atmospheric chemical species. Only the first Stokes vibrational states are considered, since the simple molecules have large vibrational energy state separation and the anti-Stokes lines are not normally populated at atmospheric temperatures. The Raman signal of a molecular species measured as a ratio to the  $\text{N}_2$  signal provides a profile which is proportional to the species vapor concentration. The  $\text{N}_2$  fraction of the atmospheric profile is known, thus the atmospheric profile of most any species, present in sufficient concentration, can be obtained. The error caused by the extinction differences between the backscatter wavelengths is small (few percent) and can be corrected using the results from multiple wavelengths.

Developments of new AOTF materials should result in extension of the useful range of the filters to the infrared spectrum where environmental applications are envisioned. The advantages in light through-put, frequency agility, ruggedness and resolution have drawn attention to this technique. The rich spectral signatures of many chemical species of interest in the infrared region from 8 to 12  $\mu\text{m}$  make it very attractive to develop the AOTF capability in this wavelength region. The AOTF instrument would provide the flexible wavelength selection needed in a lidar detector to accompany development of OPO lasers in this same wavelength region.

Table 2. LAPS lidar characteristics.

Transmitter	Continuum 9030 -- 30 Hz 5X Beam Expander	600 mj @ 532 nm 130 mj @ 266 nm
Receiver	61 cm Diameter Telescope	Fiber optic transfer
Detector	Seven PMT channels Photon Counting	528 and 530 nm -- Rotational Raman Temperature 660 and 607 nm -- Vibrational Raman Water Vapor 295 and 284 nm -- Daytime Water Vapor 277 and 284 nm -- Raman/DIAL Ozone
Data System	DSP 100 MHZ	75 meter range bins (to be upgraded to 15 m)
Safety Radar	Marine R-70 X-Band	protects 6° cone angle around beam

## 5. ARL/PSU LIDAR MEASUREMENTS

### 5.1 Water Vapor Profiles

The measurement of water vapor has been described earlier (Section 4.1). Present capabilities for water vapor measurement under nighttime conditions are thoroughly demonstrated and are fully capable of describing the water vapor profiles in the troposphere. One example of a water vapor profile is shown in Figure 1 and many others are in the earlier referenced material. This example shows one of the ways in which the lidar excels over the radiosonde balloon. In the dry layer at 2 km the balloon sensor goes into cut-off and shows a late recovery at about 3.5 km on ascent. Measurements of water vapor during the daytime have been demonstrated using 4th harmonic of the Nd:YAG laser.

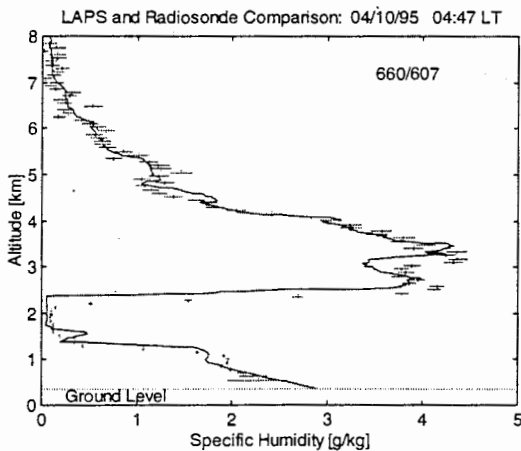


Figure 1. An example water vapor profile measured by the LAPS is lidar compared with a radiosonde balloon on 10 April 1995 at State College PA. The lidar profile shows the standard deviation of the water vapor based upon the count statistics during a 30 minute integration with no smoothing of the 75 meter measurement intervals.

At UV wavelengths, the measurements of  $N_2$  and  $H_2O$  are contaminated by the difference in absorption at the two wavelengths due to  $O_3$  in the lower troposphere (see Ref 24). However, we have found that an adequate correction can be obtained from the use of the measured Raman signals of the  $N_2$  and  $O_2$  compared to the known mixing ratio. This analysis results in a measured profile of  $O_3$  from the surface to 3 km.

### 5.2 Temperature Profiles

Rotational Raman measurements of temperature were reported by Cooney (Ref 25). A double grating monochromator was used by Arshinov, et al. (Ref 26) to measure the rotational Raman spectrum. Hauchecorne, et al. (Ref 27) and Nedeljkovic, et al. (Ref 28) demonstrated the capability to measure the temperature using narrow-band filter technology in the upper troposphere and lower stratosphere. We have demonstrated the first useful profiles of tropospheric temperature from the rotational Raman line envelop using narrow band filters (Ref 19). The molecular species of the atmosphere, principally  $N_2$ ,  $O_2$  contribute to the envelope of lines on either side of fundamental laser wavelength (Ref 29). In our case, several lines of the rotational states are measured at the 530 and 528 nm filter bands. The envelop shape is determined by the population distribution of the rotational states for the temperature of the gas in the scattering volume, which is illuminated by the doubled Nd:YAG laser at 532 nm. Rotational lines are available on both the long and short wavelength sides of the fundamental exciting frequency, however we have chosen the short wavelength side of the distribution to eliminate any excitation from fluorescent transitions. The ratio between the intensities of the two filter bands is used to directly determine the temperature. An example of the profile derived from the LAPS rotational Raman results is shown in Figure 2. Comparison of a rawinsonde balloon measurement is used to develop a calibration curve based upon an empirical fit. It is possible that the measured temperature profile and a ground based measurement of the surface pressure be used to generate the profiles of the structure properties, density, pressure and temperature based on calculations using the hydrostatic equation and the ideal gas law. The calculated profile of density can be used to obtain the  $N_2$  profile which will then place an absolute density on the water vapor from the ratio of vibrational Raman signals.

### 5.3 Optical Extinction Profiles

Optical extinction can be measured based on the molecular profile from the Raman scatter, or from a proper description of the particle size distribution using a bistatic lidar measurement. During the CASE (Coastal Aerosol Scattering Experiment) and the EOPACE (Electro-Optical Propagation Assessment in the Coastal Environment) field campaigns, the optical extinction and the scattering phase function have been

measured as a way of describing the particle size distribution and density. The first tests of this measurement technique were conducted in September 1995, during the CASE I on Wallops Island Virginia. This location was chosen for its humid and misty, coastal/marine environment, and for an unobstructed 3.28 km horizontal path over a salt marsh. The Penn State LAMP monostatic lidar was operated on both a horizontal path and pointed vertical. When operating on a horizontal path the LAMP lidar collected rotational Raman temperature profiles, vibrational Raman water vapor profiles, vibrational Raman nitrogen profiles, and bistatic aerosol/molecular scattering profiles at the fundamental laser wavelength of 532 nm.

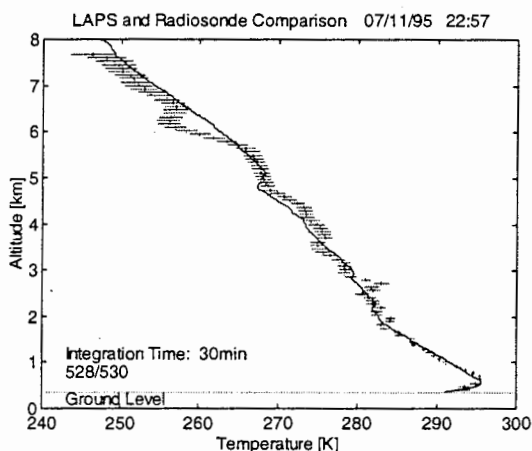


Figure 2. The temperature profile derived from the rotational Raman scatter measured by the LAPS lidar is shown with the standard deviation of the count statistics indicated.

### 5.31 Optical extinction from molecular profiles determined from Raman scatter

The previous techniques for measurements of the optical properties were limited to point sensors or path integrated transmission. The ARL/PSU lidar has been used to demonstrate that true extinction profiles can be obtained from molecular Raman scatter profiles. The approach provides a way of remotely sensing a vertical profile from the surface to 10 km. By measuring these meteorological properties together with the aerosol backscatter and extinction, the growth or dissipation phases of clouds and aerosols can be investigated.

Measurements of optical extinction are based upon gradients in the molecular profiles, using the  $N_2$  vibrational Raman or a band of the rotational Raman

lines. We have been able to demonstrate that the true optical extinction can be determined for clouds and aerosol layers. In order to calculate extinction due to aerosols from Raman lidar measurements, we take the following steps:

- 1) Apply the range correction to the backscatter Raman shifted signal.
- 2) Correct for the attenuation due to molecular scattering on the way out at 532 nm and the Raman shifted wavelength on the way back to the lidar. The molecular attenuation coefficients for 532 and 607 nm are known from the cross-sections for  $N_2$  and  $O_2$ ,

$$\alpha_{532} = 0.013 \text{ km}^{-1} \quad \alpha_{607} = 0.007 \text{ km}^{-1}$$

- 3) For the 528 and 530 nm data we can calculate the extinction value for 532 nm by fitting a least square algorithm to the following function,

$$I(R) = I_0 e^{-2\alpha_{532}R}$$

to the part of the profile that is not affected by the telescope form factor, beyond about 1 km.

- 4) The extinction of the 607 nm is obtained by fitting the function,

$$I(R) = I_0 e^{-(\alpha_{532} + \alpha_{607})R}$$

to the 607 nm profile. This algorithms can only determine the sum of the two extinctions but with the extinction determined in 3), the extinction for 607 nm can be calculated.

Figure 3 shows the variation of the optical scattering which can occur over the 3.3 km path as the air mass changes during a three hour period. The initial clear air measured at 22:34 on 17 September 1995 is replaced by an aerosol scattering air mass which is observed over about half of the path to the target board at 23:39. The increased optical scattering air mass is fairly uniform over the region by 00:39 on 18 September.

### 5.32 Optical extinction from bistatic lidar

The spherical particle scattering phase function calculated from the Mie scattering theory has obvious features which indicate high sensitivity to angle scattering function, particularly in the angle range of 150 to 175 degrees. The question of whether the distribution of realistic sizes mixed together would

remove the uniqueness of the phase function dependence upon size has been investigated. Also, the question of whether the Mie theory should apply to atmospheric measurements requires an assumed spherical shape for the particles. The coastal region, with its high humidity, is the natural region to investigate the applicability of the bistatic lidar measurement. Calculations that have been performed by Stevens (Ref 30) show that the unique character of the phase function dependence upon size is maintained when the calculation includes a realistic distribution of particle sizes. It is possible to ignore the absolute signal measurement and the sensitivity dependence on angle by using the polarization ratio. The ratio of the scattered intensity parallel and perpendicular to the measurement plane is used. By rotating the polarization plane and recording the signal on each pixel, it is possible to obtain information on the phase function dependence upon particle size based upon this ratio. The success in making these measurements has been demonstrated in recent CASE tests.

The bistatic receiver uses a linear photodiode array to image the radiation scattered from a high power CW or pulsed laser system. By observing the angular scattering variation along a horizontal path, information contained in the scattering angle phase function can be obtained. A technique has been developed to estimate particle size and distribution widths (of spherical scatters) by comparing the scattered return of laser beams polarized parallel and perpendicular to the scattering plane. A polarizer is used on the receiver to measure the cross polarization for determining the amount of multiple scattering and non-sphericity of the particles in the scattering volume.

The bistatic lidar uses the ratio obtained from the image of the scattering of two perpendicular polarization components with respect to angle, one in the scattering plane and one perpendicular to it. The use of a ratio cancels the effects of many problems, including non-linearity across the field of view of the receiver and extinction differences due to different path lengths for each scattering angle. The bistatic receiver simultaneously measures the scattering by forming an image of the backscattered radiation over an angle range of  $155^\circ$  to  $180^\circ$ . The assumption of a uniform

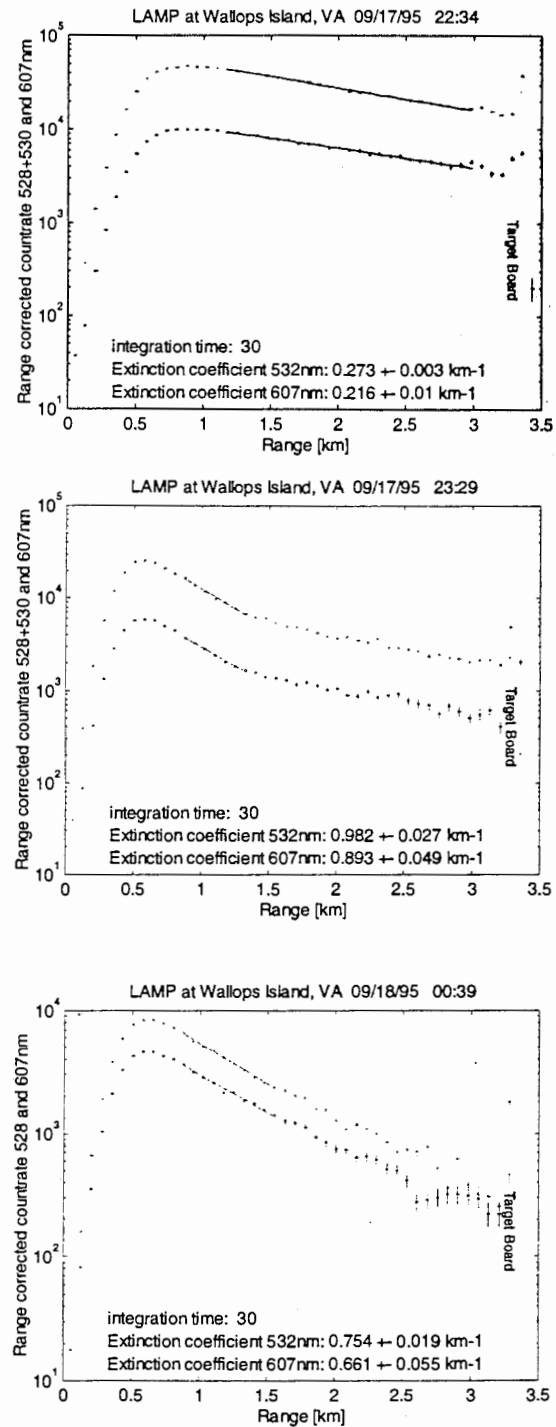
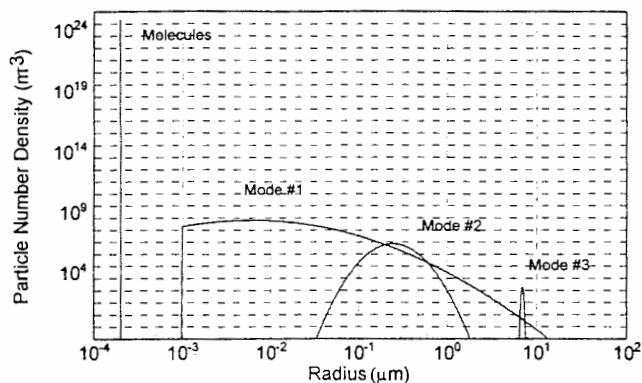


Figure 3. Optical extinction measured over a 3.3 km path at NASA Wallops Island VA on the night of 17/18 September 1995. An air mass change occurs near 23:29 when the aerosol scattering increases.

horizontal path is verified with horizontal extinction profiles from the monostatic Raman lidar during each data set. Although this polarization ratio contains the information needed to characterize the scatterers, a model is needed to relate this ratio to the desired parameters, such as extinction, and particle size distribution. The tri-modal aerosol distribution is



indicated in Figure 4.

Figure 4. A plot of a trimodal lognormal particle size distribution using the bistatic lidar model. The addition of  $2.54 \times 10^{25}$  molecules per  $m^3$  is shown at the "equivalent Mie radius" of 0.198 nm.

An example of this measurement technique is shown in Figure 5a, with the best fit of the model, and the corresponding trimodal distribution in Figure 5b. During this night, temperature decreased while the extinction increased until the wind brought a new air mass with different scatterers in the area. The second mode of the distribution was seen to narrow its distribution width as it grew from a radius of 0.166  $\mu m$  to 0.237  $\mu m$ . At the same time, the third mode increased from a radius of 6.46  $\mu m$  to 8.91  $\mu m$ . This data set is most striking because the model follows almost every contour in the data between 155° and 180° as seen in Figure 5a. Not only does the model fit the data almost perfectly, but the calculated extinction coefficients are also the same as those measured by the Raman lidar, see extinction data in Figure 5a. It is important to note that the extinction calculated from the Raman molecular extinction agrees very well with the extinction calculated for the size distribution determined from the bi-static lidar analysis, compare the values given in Figure 5a.

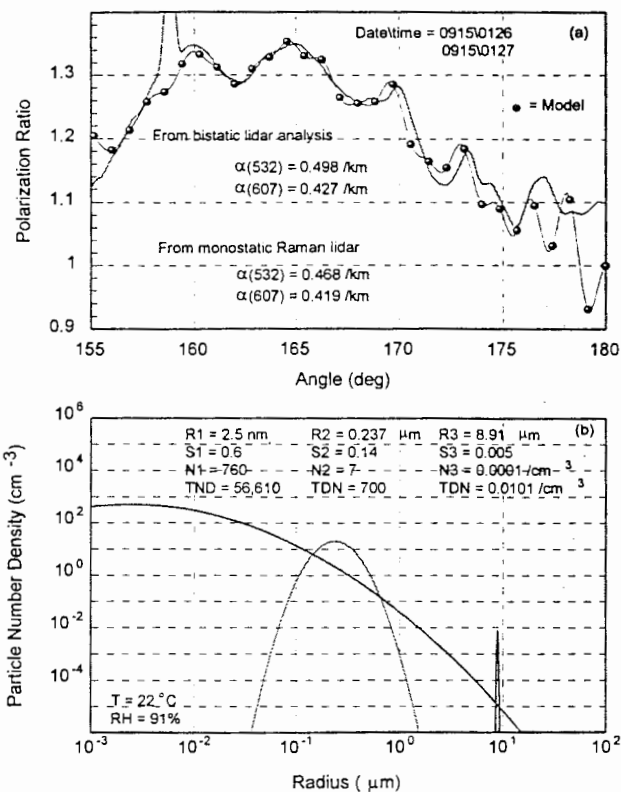


Figure 5. (a) A most convincing example of this bistatic lidar measurement technique, showing the best fit of the spherical model, using the distribution from (b), with the data. The radiation fog mean radius has grown from 6.46  $\mu m$  to 8.91  $\mu m$  in only 2.5 hours. Note the comparison of the extinction coefficients calculated from the Raman technique and from the particle size distribution which are listed in the figure.

## 6. SUMMARY

The application of laser remote sensing to measurement of the atmospheric structure properties has been demonstrated using the rotational Raman technique. Many chemical species in the atmosphere, whether these result from pollution sources, accidental release of hazardous vapor from industrial processes, or from the release of toxic chemicals in the battlefield environment, can be measured by vibrational Raman and DIAL techniques. The capabilities for active sensing using vibrational Raman scattering, DIAL (Differential Absorption Lidar), SPR-DIAL (Spectral Pattern Recognition-DIAL) have been demonstrated. Future developments with fluorescence and resonance Raman techniques should add to these capabilities. Lidar fluorescence techniques will have applications to measurements of contamination of surfaces, water columns and for

optical extinction by analyzing the molecular profiles from Raman scattering. Use of the scattering phase function with bi-static lidar measurements has shown that information on the particle size and distribution can be obtained. The progress in development of ground based techniques and the initial demonstrations of lidar on aircraft and satellites suggests that future lidars should make significant contributions to remote sensing from space based platforms, which will provide a global dimension to measurements and models.

## 7. ACKNOWLEDGMENTS

Special appreciation for the support of this work goes to J. Richter of NCCOSC NRaD, G. Schwemmer of NASA GSFC and SPAWAR PMW-185. The efforts of Savy Mathur, Paul Haris, Tom Petach, Bob Smith and Glen Pancoast have contributed much to the success of this project.

## 8. REFERENCES

1. M. P. McCormick, D. M. Winkler, E. V. Browell, J. A. Coakley, C. S. Gardner, R. M. Hoff, G. S. Kent, S. H. Melfi, R. T. Menzies, C. M. R. Platt, D. A. Randall, and J. A. Reagan, "Scientific Investigations Planned for the Lidar In-Space Technology Experiment," *Bulletin of the Am. Meteor. Soc.* 74, 205-214, 1993.
2. G. F. Tulinov, "Investigation of the Atmosphere by Ground-based and Space-based Lidars on the 'PRIDODA' Module," Report of Institute of Applied Geophysics, Moscow, Feb. 1995.
3. C. R. Philbrick, D. B. Lysak, T. D. Stevens, P. A. T. Haris and Y.-C. Rau, "Atmospheric Measurements Using the LAMP Lidar during the LADIMAS Campaign," 16th International Laser Radar Conference, NASA Publication 3158, 651-654, 1992.
4. C. R. Philbrick, D. B. Lysak, T. D. Stevens, P. A. T. Haris and Y.-C. Rau, "Lidar measurements of middle and lower atmosphere properties during the LADIMAS campaign," Proceedings of the 11th ESA Symposium, ESA-SP-355, 223-228, 1994.
5. T. D. Stevens, P. A. Haris, Y.-C. Rau and C. R. Philbrick, "Latitudinal Lidar Mapping of Stratospheric Particle Layers," *Advances in Space Research*, 13, (9)193-198, 1994.
6. P. A. T. Haris, T. D. Stevens, S. Maruvada and C. R. Philbrick, "Latitude Variation of Middle Atmosphere Temperatures," *Advances in Space Research*, 13, (9)83-87, 1994.
7. C. R. Philbrick and D. W. Blood, "Lidar Measurements of Refractive Propagation Effects," in Propagation Assessment in Coastal Environments, NATO-AGARD CP 567, Paper 3, 13 pg, 1995.
8. C. R. Philbrick and P. H. Kurtz, "Remote Sensing of Atmospheric Chemical Contamination," Proceedings of Institute of Nuclear Materials Management, 36th Annual Meeting, July 1995.
9. D. A. Leonard, R. N. Bigelow, I. K. Munson, N. T. Nomiya and H. E. Sweeney, "Remote Chemical Agent Detection and Measurement System Using a CO<sub>2</sub> Laser Radar," 1984 IRIS Speciality Group on Active Systems, Johns Hopkins University, Laurel MD, November 1984.
10. D. A. Leonard, "Observation of Raman scattering from the atmosphere using a pulsed nitrogen ultraviolet laser," *Nature* 216, 142-143, 1967.
11. J. A. Cooney, "Measurements on the Raman component of laser atmospheric backscatter," *Appl. Phys. Lett.*, 12, 40-42, 1968.
12. S. H. Melfi, J. D. Lawrence Jr. and M. P. McCormick, "Observation of Raman scattering by water vapor in the atmosphere," *Appl. Phys. Lett.*, 15, 295-297, 1969.
13. J. A. Cooney, "Remote measurement of atmospheric water vapor profiles using the Raman component of laser backscatter," *J. Appl. Meteor.*, 9, 182-184, 1970.
14. J. A. Cooney, "Comparisons of water vapor profiles obtained by rawinsonde and laser backscatter," *J. Appl. Meteor.*, 10, 301, 1971.
15. H. Inaba and T. Kobayasi, "Laser-Raman Radar," *Opto-electronics*, 4, 101-123, 1972.
16. G. Vaughan, D. P. Wareing, L. Thomas and V. Mitev, "Humidity measurements in the free troposphere using Raman backscatter," *Q. J. R. Meteorol. Soc.*, 114, 1471-1484, 1988.
17. S. H. Melfi, D. Whiteman and R. Ferrare, "Observations of atmospheric fronts using Raman lidar moisture measurements," *J. Appl. Meteor.*, 28, 789-806, 1989.
18. D. N. Whiteman, S. H. Melfi and R. A. Ferrare, "Raman lidar system for the measurement of water vapor and aerosols in the Earth's atmosphere," *Appl. Optics* 31, 3068-3082, 1992.
19. C. R. Philbrick, "Raman Lidar Measurements of Atmospheric Properties," in Atmospheric Propagation and Remote Sensing III, SPIE Volume 2222, 922-931, 1994.

20. W. B. Grant, "Differential absorption and Raman lidar for water vapor profile measurements: a review," *Optical Engineering*, 30, 40-48, 1991.
21. R. M. Measures, Laser Remote Sensing, Krieger Publishing, Malabar FL, 1992.
22. V. I. Pustovoi and V. E. Pozhar, "Collinear Diffraction of Light by Sound Waves in Crystals: Devices, Applications and New Ideas," *Photonics and Optoelectronics* 2, 53-69, 1994.
23. F. L. Vizen, Yu. K. Kallinikov and V. I. Pustovoi, "Quartz Acousto-Optic Filter," *Scien. Inst. and Exp. Tech.* 6, 170, 1979.
24. D. Renaut, J. C. Pourny and R. Capitini, "Daytime Raman-Lidar Measurements of Water Vapor," *Opt. Lett.* 5, 233, 1980.
25. J. Cooney, "Measurement of atmospheric temperature profiles using the Raman component of laser backscatter," *J. Appl. Meteor.* 11, 108-112, 1972.
26. Yu. F. Arshinov, S. M. Bobrovnikov, V. E. Zuev and V. M. Mitev, "Atmospheric temperature measurements using a rotational Raman lidar," *Appl. Optics* 22, 2984-2990, 1983.
27. A. Hauchecorne, M. L. Chanin, P. Keckhut, and D. Nedeljkovic, "Lidar monitoring of temperature in the middle and lower atmosphere," *Appl. Phys.* B55, 29-34, 1992.
28. D. Nedeljkovic, A. Hauchecorne and M. L. Chanin, "Rotational Raman lidar to measure the temperature from the ground to 30 km," *IEEE Trans. Geos. Remote Sens.* 31, 90-101, 1993.
29. P. A. T Haris, "Pure Rotational Raman Lidar for Temperature Measurements in the Lower Troposphere," Dissertation, Department of Electrical Engineering, Penn State University, 1995.
30. T. D. Stevens, "Bistatic Lidar Measurements of Lower Tropospheric Aerosols," PhD Dissertation, Department of Electrical Engineering, Penn State University, 1996.